

Molecular Insights into Dissolved Organic Matter in Natural Dew Water: Biograde Films on Leaf Surfaces

Monica Dibley, Aron Jaffe, and Rachel E. O'Brien*



Cite This: *ACS Earth Space Chem.* 2022, 6, 775–787



Read Online

ACCESS |

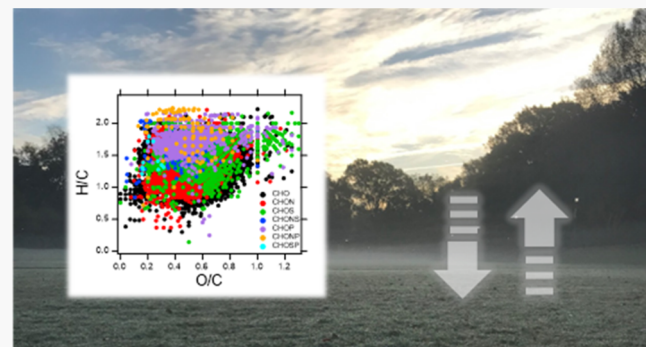
Metrics & More

Article Recommendations

Supporting Information

ABSTRACT: Dew water serves as a temporary reservoir of dissolved organic molecules that are released in the morning when the dew evaporates. Many locations allow for direct sunlight on the dew water in the morning, raising the possibility for photolysis-driven chemical reactions. The majority of prior works looking at dew water chemical composition has targeted freshly deposited dew on clean surfaces like Teflon. However, the dissolved organic material in dew is a mixture of compounds deposited during the night, as well as water-soluble compounds already present on the surface. Here, we analyzed six separate dew or frost water samples collected off grass and bush leaf surfaces in Southeast Virginia in the fall of 2020 and found evidence for a water-soluble surface grime layer that we term biograde. The chemical composition and photoactivity of the mixtures were probed using Fourier transform ion cyclotron resonance mass spectrometry, offline-aerosol mass spectrometry, and UV/vis spectroscopy. Complex organic mixtures were found in all the samples with a total of ~9600 identified molecular formulae containing C, H, N, O, S, and P. Many samples had strong absorption in the visible region, and all showed an initially rapid photodecay. The composition varied between samples with possible sources including plant guttation and microbial waste as well as deposition of atmospheric organic aerosol particles, soil particles, and fog droplets. The composition of organic molecules, combined with their photoactivity, suggests that dew water may be a complex source for water-soluble gases as it evaporates.

KEYWORDS: organic film, dew water, deposition, metabolites, FT-ICR, photolysis



1. INTRODUCTION

The biosphere is an important source for reactive organic carbon (ROC) compounds that fuel atmospheric chemistry.^{1,2} Many of these organic chemicals are emitted directly from plants, termed biogenic volatile organic compounds (BVOCs) and, once in the atmosphere, they can be oxidized by ozone, OH radicals, nitrate radicals, etc.³ In many cases, this chemistry involves the addition of oxygen functional groups to the molecules, lowering their vapor pressure to the extent that they may condense onto existing aerosol surfaces or nucleate to form new aerosol particles.⁴ Aerosol particles formed in this manner are termed secondary organic aerosol (SOA).⁵

The total flux of BVOCs and SOA out of any portion of the biosphere will depend not only on the emission and formation rates but also on the deposition rate because semivolatile biogenic organic compounds (SVOCs), oxidized VOCs, and SOA particles can deposit onto surfaces like leaves, stems, trunks, and roots in the biosphere.^{6,7} The deposition of VOCs and SVOCs is important to understand because it may play a role in the total aerosol budget; models show that including dry deposition of oxidized VOCs onto surfaces will decrease the SOA predicted to form by ~50%.⁸ In addition, after

deposition, equilibria can be established, leading to biosphere surfaces potentially serving as non-permanent sinks for ROC. This can be especially true if the nature of the surface changes, as happens when surface water films and dew are present at night but then evaporate during the day.⁹

Beyond equilibrium exchange, the surfaces may also act as a reactive site for the formation of new VOCs. Depending on the type of chemical reaction, the chemical identity of the “revolatilized” ROC may differ compared to what was originally deposited. This presents a challenge in interpreting fluxes in the biosphere because volatile reaction products may have different diurnal patterns compared to direct leaf emissions. Their formation will also depend on environmental factors such as the temperature, surface wetness, and pH of the surface water. Finally, the emissions will also be affected by the

Received: December 26, 2021

Revised: February 2, 2022

Accepted: February 4, 2022

Published: February 15, 2022



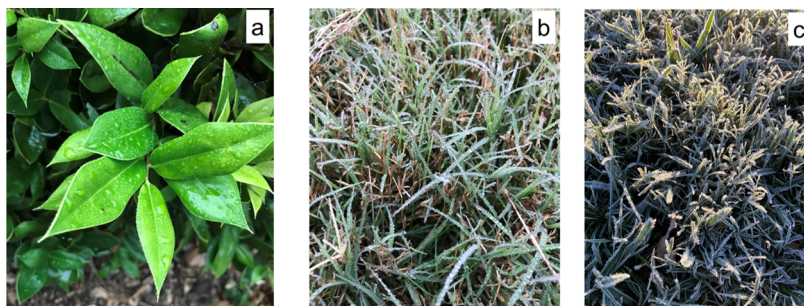


Figure 1. (a) Image of the bush taken before sample collection, (b) image of grass on the William and Mary campus during a heavy dew fall morning, and (c) image of grass prior to collection of the frost sample.

composition, reactivity, volatility, and water solubility of the deposited and newly formed ROC.

Here, we term the film that forms on biosphere surfaces “biogrime,” in analogy to the “urban grime” surface films that have been characterized in cities.^{10–12} Urban grime is a mixture of dust, metals, inorganic ions, and trace organic compounds and comes from dry deposition of particles and SVOCs onto city surfaces.^{12,13} In contrast, the area in which these dew water samples were collected has less urban influence, and leaf surfaces were sampled. Biogrime includes deposited materials but can also include materials from plants along with microbial and fungal waste. This organic mixture can serve as a reactive site for the emission of new ROCs as the components in the film age as well as serving as a possible food source for microbes, which can themselves directly emit VOCs.^{14,15} The films may also be a reactive site for the transformation of inorganic compounds into oxidants, as has been observed for the formation and emission of HONO off surfaces.^{16–18}

Biogrime’s role in an ecosystem will depend on its chemical composition. Biogrime films on leaf surfaces in forests have been investigated in throughfall experiments where rainwater that has washed through the canopy is collected and analyzed.^{19–23} Complex organic mixtures were observed in these samples, with some evidence for longer range transport and deposition of anthropogenic organic aerosol particles.²⁰ Other studies imaged deposited particles on clean substrates and show large biological particles including fungi and bacteria.^{24,25} Throughfall experiments provide a good perspective on biogrime as they target tree leaf surfaces, but a more complete picture of the composition of natural biogrime across different ecosystems is needed, as well as a comparison between dry surface films and wet surface films such as dew water.

Dew forms on cool, clear, calm nights when surface temperatures drop below the dew point by radiating heat into the cloudless sky.²⁶ Dew water will usually start forming after nightfall and surface water films can remain for multiple hours into the morning before evaporating as the temperature warms. Frost formation can follow a similar pattern, where if the temperature is low enough, the water freezes on surfaces. The chemical composition of dew water is a mixture of gas-phase and particle-phase materials that deposit into it during the night, in addition to any water-soluble portion of biogrime already present on the surface that dissolves.

Previous studies on organic matter in dew water have mostly involved samples collected on clean surfaces like Teflon or stainless steel.^{27–30} This measures ROC from gases and organic aerosol particles that deposit into the surface films

during that night, but it does not provide any information on the mixture of water-soluble chemicals already present on natural surfaces. Depending on the chemical composition of the biogrime, there may be differences in the solubility and reactivity of chemicals that deposit into the dew water. For example, previous work showed enhanced dissolution of hydrophobic VOCs, possibly due to the solubilizing effect of humic-like substances into the dew water.^{31,32} Chemical reactions may be especially prevalent in the morning when dew water droplets evaporate and can be simultaneously exposed to sunlight, both of which are known to drive chemical transformations in aerosol organic matter.^{33,34}

Here, we collected dew and frost water samples off natural surfaces including grass and bush leaves in Southeast Virginia to probe the chemical composition of the water-soluble material in biogrime. The samples contained a complex mixture of organic compounds, with approximately 9600 molecular formulae identified across six samples using Fourier transform-ion cyclotron resonance mass spectrometry (FT-ICR-MS). The molecular formulae measured with FT-ICR and the chemical characteristics measured with offline-aerosol mass spectrometry (AMS) suggest multiple different sources for the films including the material exuded from plants, from microbes/fungi, deposited soil particles, marine influenced aerosol particles, and fog droplets. The mixtures were also photoactive, suggesting that chemicals present could drive aqueous photochemical reactions in the morning, before the dew droplets completely dry. This work is the first comprehensive investigation of the complex organic mixtures present in dew water on natural surfaces and shows that these biogrime films have a wide range of sources and an evolving chemical composition.

2. MATERIALS AND METHODS

2.1. Sample Collection and Preparation. Samples were collected off natural surfaces including grass or bush leaves in and around Williamsburg, VA, in fall 2020 (Figures 1 and S1). Samples were collected from the William & Mary Campus in Colonial Williamsburg and in Sussex which is ~36 miles from William & Mary. The range of locations and surfaces was selected to provide comparisons in terms of vegetation type and location. All samples were collected using a metal spatula that was gently pulled across the surface of the wet leaves. The water that pooled in the spatula was tipped into a sample collection container, and this process was repeated until ~10–15 mL of water was collected. One sample was collected from grass that had a frozen water surface film (frost or rime) (Figure 1c). For its collection, the frost was gently dragged off the grass leaf surface with the metal spatula and collected in the

vial in the same manner as the dew. A gentle motion was used to minimize the damage to the leaf surface and thus extraction of interior portions of the plant. No changes in appearance were observed except for the removal of the dew water or frost from the leaves. The metal spatulas were thoroughly rinsed with Milli-Q water (Millipore Sigma, 18 Ω) before use, and the glass sample containers were baked at 400 °C for 6 h to remove organic material. During collection, nitrile gloves were worn on the collecting hand. Samples were filtered through a 0.2 μm Teflon filter (Thermo Scientific, 0.2 μm PTFE Membrane) as soon as possible after collection (within 10–30 min) to remove microbes. The extract material was then closed in the vial, and the sample was frozen for storage before subsequent analysis.

A table listing conditions for the sample collection is provided in the Supporting Information (Table S1). The lowest temperature, on the night of the frost sample, was 30 °F. Fog was also reported that night, so the type of ice is not known (e.g., rime ice or hoar frost) and will be termed “frost” here for simplicity. Three other collection mornings also had fog present at the ground level, and two samples were collected shortly after rainfall (Bush and Sussex). The two Sunken Garden samples were collected from different areas of the same field on the campus of William & Mary on two different dates. All samples were collected off grass except for the Bush sample (Figure 1a). During collection, some loose plant material was also often collected (i.e., small dead fragments of grass leaves). This material was removed with the filter that was used immediately after sample collection to remove bacteria. After filtration, samples had a range of colors from yellow/brown to transparent.

After thawing, some samples had a trace amount of material that did not stay in solution. This precipitate has not yet been characterized, but it was not crystalline. This material was removed before subsequent sample preparation by a second round of filtration. For each sample, four aliquots were separated out to measure the pH and UV/vis, FT-ICR, and offline AMS spectra. Measurements of pH were carried out using a Hatch HQ11D pH meter on 2.5 mL of the sample. For UV/vis analysis, ~1–2 mL fractions of the sample were diluted with Milli-Q water as needed to generate solutions that were optically transparent enough for the measurements. The need for dilution was due to the concentration of the absorbing chemicals in the solution, there were no observed precipitates present during UV/vis analysis. For MS analysis with FT-ICR, ~7–10 mL of the sample was extracted and desalting using cartridges filled with styrene divinylbenzene copolymer (Agilent Bond Elut PPL, 500 mg). Samples were loaded onto the cartridges, washed with ~2 mL of Milli-Q water, and then eluted with ~2 mL of methanol. This extract of dissolved organic matter (DOM) was then dried under ultrapure nitrogen and shipped on ice to the Cosmic Lab at Old Dominion University for FT-ICR analysis. The extraction of aqueous dissolved organic mixtures with PPL cartridges will lead to a fractionation of the sample, but this preparation has been demonstrated to provide high quality samples for FT-ICR analysis.^{35–37} For MS analysis with offline-AMS, approximately 50 μL of dew water samples was used to nebulize into a high resolution (HR)-time of flight (ToF)-aerosol mass spectrometer³⁸ using the small volume nebulizer (SVN).³⁹ An internal standard was added for quantification, but no other sample preparation was used to enable direct comparison with the UV/vis measurements.

2.2. MS Analysis. FT-ICR analysis was performed at Old Dominion University in the COSMIC lab on a Bruker Daltonics 12 Tesla Apex Qe FT-ICR mass spectrometer in negative ion mode using an Apollo II electrospray ionization (ESI) source. Methanol was used to reconstitute the sample, and mass spectra were collected in the range of m/z 100–2000. Mass spectral peaks were picked using DeCON 2LS (<https://pnnl-comp-mass-spec.github.io/DeconTools/>) with a peak to background ratio of 5 and a signal to noise threshold of 3. An internal calibration was carried out using carbon-, hydrogen-, and oxygen-containing peaks, and then peaks were picked in the range of $\text{C}_{0–100}\text{H}_{0–200}\text{N}_{0–5}\text{O}_{0–100}\text{S}_{0–3}\text{P}_{0–1}$ within a ± 1 ppm window using the Molecular Formula Calculator v1.1 (<https://nationalmaglab.org/user-facilities/icr/icr-software>). 2D Kendrick mass series (CH_2 and H_2) in combination with a 1D Kendrick of oxygen were used to assign peaks. A threshold assignment was applied to the samples with DBE steps greater than five ruled as too large to be classified within the same 2D Kendrick family. Two blanks were generated, one using Milli-Q water and the other using Milli-Q water run over the same type of nitrile gloves used for collecting the dew water. Both blanks were prepared with the PPL cartridges. Any peaks within ± 3 ppm of a blank peak were removed. Additional cleaning was carried out by removing any peaks that do not match bonding criteria for organic compounds: $\text{O/C} > 1.9$, $0.33 < \text{H/C} < 2.25$, $\text{N/C} > 0.5$, $\text{S/C} > 0.2$, $\text{P/C} > 0.1$, and $(\text{S} + \text{P})/\text{C} > 0.2$.⁴⁰ Here, a slightly larger threshold for O/C than that for previous work was used, due to the possible presence of phosphates on sugars. A total of 9958 molecular formula were identified across all the samples. Double bond equivalence (DBE) was calculated using

$$\text{DBE} = 1 + \frac{1}{2}(2\text{C} - \text{H} + \text{N} + \text{P})$$

Statistical analysis was carried out using hierarchical clustering with the Wards method⁴¹ using IBM SPSS. The peak intensities (z) were standardized using

$$z = \frac{x - \mu}{\sigma}$$

where x is the peak intensity, μ is the average intensity of the mass spectrum, and σ is the standard deviation in peak intensity within the sample.²⁰ If no peak was present, the intensity was set to 0 prior to standardization.

Offline AMS analysis was performed by nebulizing samples into an HR-ToF-AMS instrument using the SVN.³⁹ An internal standard containing ~0.25 g/L isotopically labeled ammonium nitrate ($\text{NH}_4^{15}\text{NO}_3$) and ~0.25 g/L ammonium iodide was mixed with the samples (~50/50) prior to nebulization to enable quantification. Three replicate injections were performed for each sample, and the glove blank was used. All samples were run without solid-phase extraction. The data were processed using Igor 7, ToF-AMS Analysis Toolkit 1.62A, and HR Analysis 1.22A. For elemental ratios, the average mass spectrum was calculated and the Improved-Ambient correction was used.⁴²

2.3. UV/Vis Spectroscopy and Photolysis. UV/vis spectra were collected using a PerkinElmer LAMBDA 35 UV/vis spectrometer with a quartz cuvette (Thorlabs). Spectra were collected from 200 to 800 nm, and samples were diluted as needed with Milli-Q water to produce spectra with absorbance less than 1.5 across the full spectrum (230–800 nm). Photolysis was carried out by placing quartz cuvettes ~14

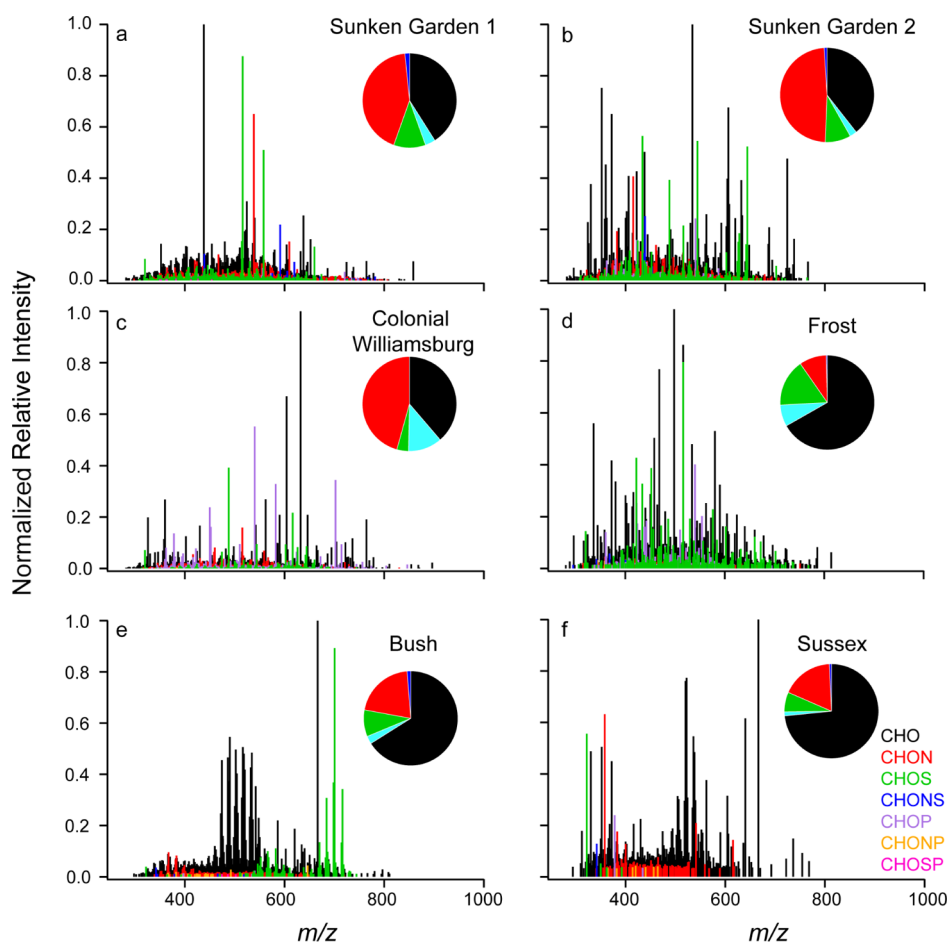


Figure 2. Mass spectra for dew water extracts colored by the molecular formula type (key bottom right). Inset pie charts show the relative number of each type, with the three phosphorus-containing compounds combined into one color (light blue) to aid visualization. The colors for the other classes match between the mass spectra and pie charts.

cm away from the front of a xenon arc lamp (Figure S2). Photobleaching was tracked by measuring the absorption at semiregular intervals over ~ 50 h, and photolysis rates were fit from the decay in the average signal from 360 to 365 nm using a biexponential fit

$$y = A_1 e^{-t/\tau_1} + A_2 e^{-t/\tau_2}$$

where t is the time in front of the xenon arc lamp and τ is the lifetime for photodecay.

3. RESULTS AND DISCUSSION

3.1. Molecular Characterization of DOM in Natural Dew Water. Detailed characterization of the molecular composition of DOM in dew water samples can provide information on the types of sources contributing to biogrime. DOM was measured in each sample with negative ion mode ESI and FT-ICR MS after solid-phase extraction. Ions observed with negative ion mode ESI have functional groups like carboxylic acids and alcohols which have weakly bound protons that can be removed to form the negative ions. Figure 2 shows FT-ICR mass spectra for each of the dew water samples with the peaks colored according to the elements present in the identified molecular formula. The inset pie charts show the total number of unique molecular formula identified for each ion type; for clarity, all phosphorus-containing molecules were combined into one color (light

blue). In all samples with larger numbers of phosphorus-containing compounds (Figure 2a–d), CHOP contributed more than 80% of phosphorus-containing molecular formulas, making them the largest contribution to the light blue wedges in the pie charts (Table S2), and possible sources for these ions are discussed below. Ions were observed between ~ 200 and 800 m/z , and the dominant chemical classes for most of the samples were compounds containing carbon, hydrogen, and oxygen (CHO, black) and/or those containing carbon, hydrogen, oxygen, and nitrogen (CHON, red). The frost sample contained slightly higher numbers of CHOS (green) than CHON compounds (Table S2). The higher number of CHOS compounds in this sample has an unknown source but may indicate differences in the soil that deposited to form the biogrime. Future work is needed to determine the sources for the CHOS compounds in different biogrime samples.

In general, a higher intensity in the ESI mass spectrum does not directly correlate to a larger relative abundance due to matrix effects. However, the observed intensity distributions suggest differences in the chemical composition of the mixtures collected shortly after rainfall compared to the rest of the samples. Samples collected off grass in Williamsburg (Figure 2a–c) and the frost sample (Figure 2d) have a broad distribution of peaks with different ion types distributed relatively evenly across the mass range. The broad intensity distribution observed in the top four mass spectra (Figure 2a–d) is similar to distributions observed for complex organic

Table 1. Parameters for the Six Dew Water Samples^a

sample name	sample date (2020)	pH	rain/fog ^b	# formula	N_c	O/C	H/C	N/C	mass (amu)
Sunken Garden 1	Oct. 22	6.1	N/Y	6115	24	0.47	1.4	0.031	511
Sunken Garden 2	Nov. 5	6.5	N/Y	4525	22	0.52	1.5	0.045	493
Colo. Williamsburg	Nov. 11	6.0	N/N	4666	23	0.51	1.6	0.044	518
Frost	Nov. 19	5.8	N/N	2622	21	0.65	1.4	0.0051	508
Bush	Oct. 27	5.3	Y/Y	1738	27	0.35	1.5	0.0060	520
Sussex	Oct. 26	5.5	Y/Y	737	24	0.39	1.6	0.0096	469

^aElemental ratios, number of carbons (N_c), and average molecular weight (atomic mass units) are all intensity-weighted averages from the FT-ICR data.

^bY for rain indicates rainfall occurred 1 day prior to collection and Y for fog indicates fog during collection.

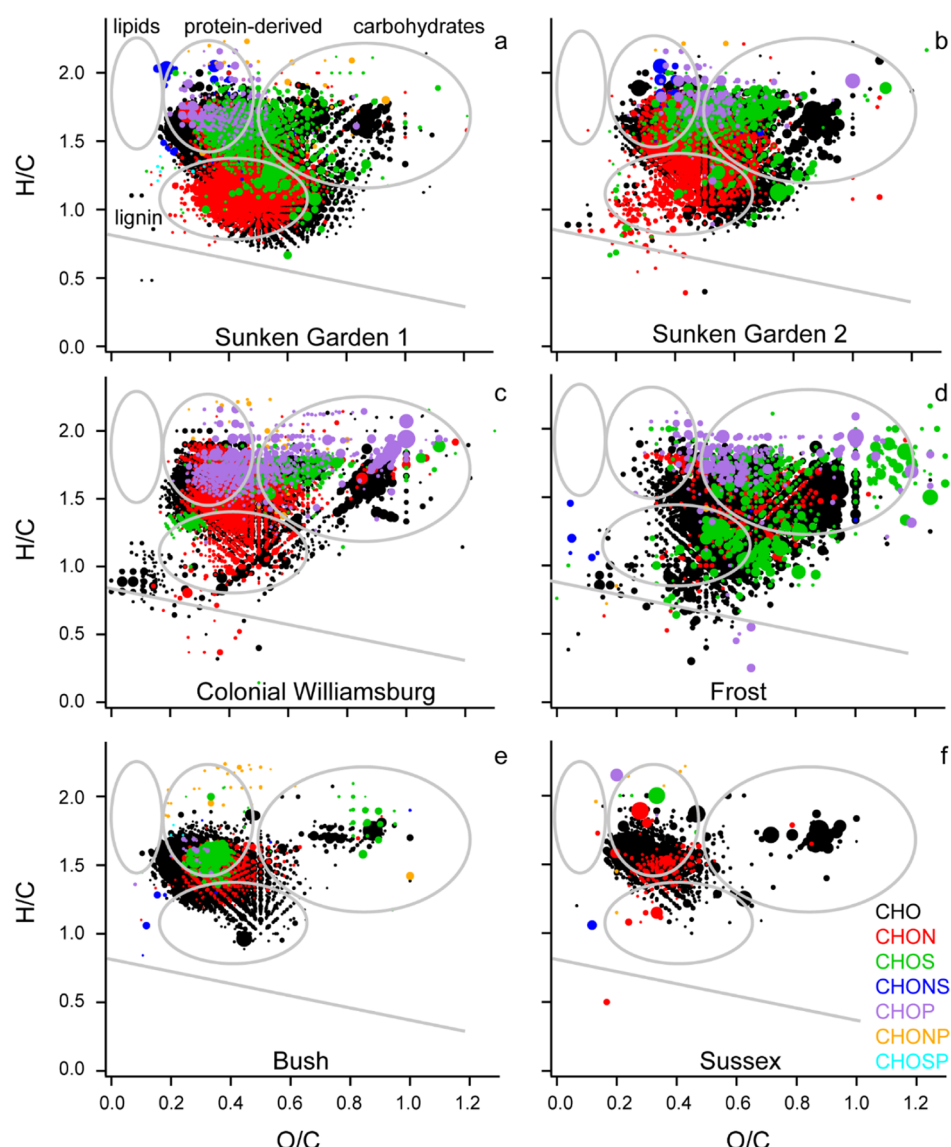


Figure 3. Van Krevelen diagrams for dew water extracts colored by the molecular formula type. The markers are sized by the log of the intensity, and the colors correspond to the molecular formula type. Approximate ranges for different compound classes are given as gray circles with labels in (a). Compounds below the solid line correspond to condensed aromatics.

mixtures found in some soil organic matter extracts.^{35,43,44} In contrast, the samples collected off the bush and in Sussex (Figure 2e,f) were collected shortly after rainfall and both had fog in the morning. These samples show fewer peaks overall (Table 1) and more clustering of the peaks with a central CHO distribution around 500 m/z (black). The narrower intensity distributions observed for the CHO compounds in Figure 2e,f are more similar to the intensity distributions

observed for oligomers found in aerosol particles and suggest that the mixtures have a larger contribution from dry deposited aerosol particles or occult deposition of fog droplets.^{45–47}

All of the samples had pH values between ~5.3 and 6.5 (Table 1). These values are in the same range as reported for dew collected off clean surfaces around the world.^{28,29,48–51} The pH values here were measured after samples had been filtered, frozen, and melted again, so there may be small

changes compared to values measured for droplets in the field. The pH of the dew may be influenced by partitioning of ammonia, and it may change as the dew droplets evaporate in the morning. Future work will target pH measurements of dew droplets *in situ* in the morning to evaluate this. Lower pH values were measured in the cleaner samples (Bush and Sussex), which also had fog during the morning. The pH range for fog water can be lower than dew water,^{28,52} suggesting that these samples may have more influence from occult deposition of fog or less influence from more basic components of soil, or both.

Additional insights into the types of chemicals found in the mixtures can be observed in the van Krevelen plots in Figure 3. Prior work on DOM samples has shown that specific types of chemicals are typically observed in certain regions of the van Krevelen space. For example, carbohydrates tend to fall at higher O/C and H/C values, and chemicals with structures like lignin fall in the middle.⁵³ Approximate ranges for these chemical classes are indicated by overlaid ovals with labels in Figure 3a. All ions within an oval do not necessarily belong to that compound class, but they have elemental ratios that match that type of compound.

Figure 3a–c shows data from dew water collected off grass in the Williamsburg area. All three samples show many CHO and CHON compounds that fall in the same van Krevelen space centered around lignin, with some ions at the edges into carbohydrates and proteins. The large number of peaks in the lignin range suggests that the water-soluble portion of deposited soil particles may contribute to the organics in these films. Some CHON peaks also fall in the protein region of the van Krevelen space, and some of these also have molecular formula consistent with small peptides. The presence of intact proteins was not observed in the mass spectrum, but the trace insoluble material that was found after the freeze/thaw cycle during sample preparation could correspond to protein aggregates or other cellular materials.

The O/C values for the CHON compounds and many of the CHOS compounds are generally lower than what is observed for negative ion mode ESI mass spectra for aerosol particles that contain organosulfates and organonitrates.^{54,55} The lower O/C here suggests that the dew water CHON compounds may contain more reduced nitrogen functional groups like amines or imines. For the lower O/C CHOS compounds, many may be reduced sulfur, or if these are sulfate or sulfonate groups, they are formed on organic precursors with a lower initial O/C.

All samples, but especially the top four (Figure 3a–d) show the presence of phosphorus-containing ions (CHOP, purple; CHONP, orange). As mentioned above, the CHOP ions are the dominant form of phosphorus-containing compounds. This suggests that intact DNA, which would be expected to contain both nitrogen and phosphorus (CHONP), was not a large fraction of the ionized chemicals. Two main groups of CHOP ions are observed, one at a lower O/C in the region of the “protein derived” oval and one at a higher O/C in “carbohydrates.” It is likely that these are predominantly coming directly from plant materials or microbes on the plants. The CHOP ions at a lower O/C do not contain nitrogen and are thus not from proteins/peptides. Instead, they could correspond to phospholipid fragments as they have only slightly higher O/C than the lipids. Some of these ions are in the same mass range as observed for negative ion mode ESI of *Escherichia coli*,⁵⁶ but others are observed at a lower *m/z* than

expected for intact phospholipids, suggesting fragmentation, possibly due to aging on the leaf surface. The CHOP ions in the carbohydrate region may be from the photosynthesis process which uses phosphorus in multiple steps and could reach the plant surface via guttation, where xylem or phloem sap is exuded when there is increased water pressure at the roots and the stomata are closed at night.⁵⁷

The bottom two spectra (Figure 3e,f) are from samples collected after recent rainfall and show a smaller range of elemental ratios. Both spectra show a cluster of ions in the carbohydrate region with the majority falling at lower O/C and H/C ratios, close to lignin. These ions may be from deposited soil, residual organics left on the surface after the rain dried, or they may be from deposited organic aerosol particles or fog droplets, as suggested by the patterns in the intensity discussed above (Figure 2e,f). Given that many of the peaks are in the same region of the van Krevelen space as the other samples, it is also likely that soil particles and guttation are additional sources, but there is less of that material on the surfaces. The overall smaller number of ions in the samples collected after rainfall suggests that many of the compounds found in the other samples build up on the leaf surface over time, and that some of this material may wash away with rain.

Only 255 molecular formulae are common across all the samples, indicating a large variety of chemicals in the mixtures. However, hierarchical clustering shows greater degrees of similarity between certain groups of samples. Figure 4 shows

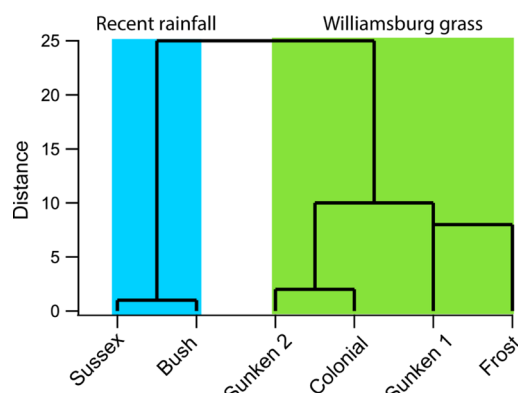


Figure 4. Dendrogram from hierarchical clustering of the FT-ICR data sets using Ward Linkage.

the dendrogram for these samples with a higher degree of similarity between the two samples collected after recent rainfall (Bush and Sussex) and a similar composition between the two samples collected in November in Williamsburg (Sunken Garden 2 and Colonial Williamsburg). These two samples were not collected in the same field, and the sample collected in the same field a month earlier (Sunken Garden 1) has a lower degree of similarity compared to those two. The frost sample is also more similar to the other grass samples than to the recent rainfall samples. In general, there are two main groups: samples that have had time to build up a film versus samples collected shortly after rainfall. This is also consistent with the visible differences in the spectra shown in Figures 2 and 3. In the future, a wider range of samples, covering more locations and times after rainfall, will provide additional insights into the sources and chemical variability present in biogeochemical processes.

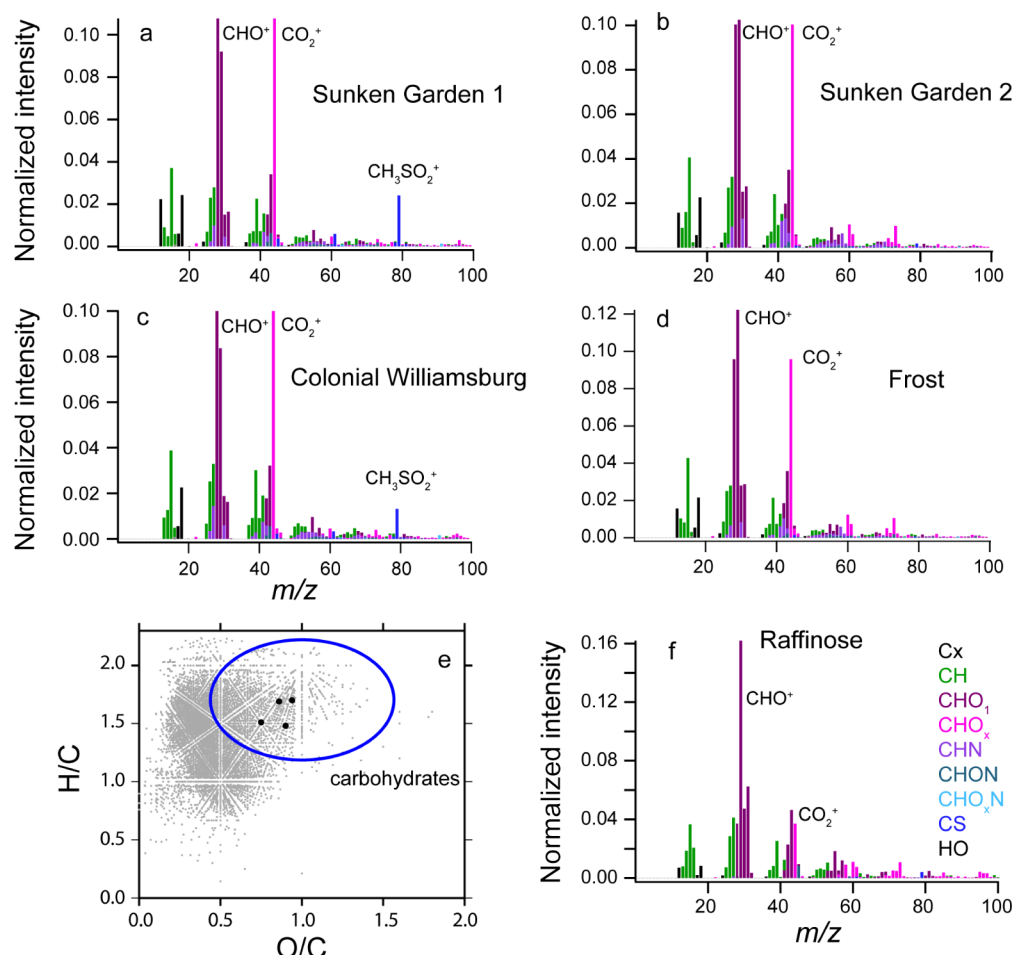


Figure 5. Offline-AMS spectra for the four more concentrated samples (a–d) as well as a raffinose standard (f). The data are colored by the type of fragment ion. (e) van Krevelen space for the full FT-ICR data set (small gray circles) with the average elemental ratios from the offline AMS spectral data overlaid on top (solid black circles); the range for carbohydrates is included (blue circle).

Taken together, all of the characterizations of the FT-ICR data sets (Figures 2–4) show that biogrime in the dew water samples appears to have three to four dominant sources: deposited soil, plant sap/microbial waste, and deposited organic aerosol particles/fog droplets. These different sources will have different accumulation rates in the film. Metabolites, amino acids, peptides, and other biological materials can come from microbes and fungi on the leaf surfaces or be exuded from the plant. Sugars and proteins in the sap may remain on the leaf surface after the guttation droplets dry. Dry deposition of soil particles in addition to organic aerosol particles and occult deposition of fog droplets onto the surfaces is likely another important source for the biogrime. Soil and organic aerosol particles will have different size distributions with different total mass and will also deposit on the surface at different rates.^{7,58} Depending on the wind speed, soil moisture, and sources for organic aerosol particles and fog droplets, there will likely also be differences in the times when each of these are the dominant mass components depositing. Taken together, the composition of organic materials on leaf surfaces appears to be dynamic and appears to be dominated by soil dust and plant/microbe waste for surfaces that have not been freshly washed by rainfall.

3.2. Offline-AMS Spectral and Chemical Characteristics.

The previous section focused on organic materials in dew water prepared using solid-phase extraction. This method

is widely used for DOM analysis and provides a sample mixture that can electrospray well for FT-ICR analysis.^{35,36,44} However, this sample preparation is not expected to extract all materials in the sample at the same efficiency.⁵⁹ Given that ESI of complex mixtures without a prior separation is not quantitative, the data discussed above provides a limited perspective on the concentrations of different chemicals present in the mixture. For a more quantitative view on the composition of the starting material, we used offline-AMS. In this instrument, pyrolysis/EI generates mass spectra for all non-refractory materials in the sample. Here, SVN-AMS was used to nebulize the samples into the instrument because of the limited sample volume. This technique has a lower concentration limit of ~ 0.1 g/L organic for aqueous samples.³⁹ The organic concentrations in the two cleaner samples (parts e and f in Figures 2 and 3) were below this cutoff, and the following discussion will focus on the four more concentrated samples.

Figure 5 shows offline-AMS spectra for the top four samples from Figures 2 and 3. AMS is a quantitative technique, and fragmentation patterns can be compared to standards to determine the dominant components present in the mixtures. In Figure 5a–d, the dominant ions in all four spectra are CO₂⁺ (m/z 44), CHO⁺ (m/z 29), and CO⁺ (m/z 28). The CO⁺ ion has an overlap in mass with N₂, so it is set to be equal to CO₂⁺ during analysis and will not be discussed further. Two samples

Table 2. Elemental Ratios from AMS Measurements as Well as Concentrations Measured by AMS^a

sample name	O/C	H/C	N/C	OM/OC	[organic] g/L	[chloride] g/L
Sunken Garden 1	0.90	1.5	0.045	2.3	0.20 ± 0.02	0.047 ± 0.003
Sunken Garden 2	0.86	1.7	0.062	2.3	0.52 ± 0.04	0.025 ± 0.002
Colo. Williamsburg	0.75	1.5	0.052	2.1	0.24 ± 0.05	0.012 ± 0.003
Frost	0.94	1.7	0.045	2.4	0.43 ± 0.08	0.014 ± 0.003

^aErrors on the concentration measurements are the standard deviation of three replicate injections.

(a and c) also show a strong fragment intensity at CH_3SO_2^+ (*m/z* 79), which will be discussed further below. The high intensity of CO_2^+ in the dew water samples suggests the presence of oxidized functional groups like carboxylic acids. Figure 5f shows the offline-AMS mass spectrum for a trisaccharide, raffinose. The highest intensity ion from the sugar is CHO^+ , and this ion has been previously linked to OH groups.⁴² The relatively high intensity CHO^+ ion in the dew water samples suggests that sugars/carbohydrates may be a large mass fraction of the mixture. This also matches the O/C and H/C average ranges for the samples, which fall in the carbohydrate region of van Krevelen space (Figure 5e). The relatively lower observed intensity for sugars/carbohydrates in the FT-ICR data sets (Figures 2 and 3) is likely due to a lower extraction efficiency and a lower ionization efficiency in the negative ionization mode, especially compared to chemicals with acid functional groups in the mixture.

The AMS spectra also show intensity at CH_3SO_2^+ (*m/z* 79) for Sunken Garden 1 and Colonial Williamsburg (Figure 5a,c). This ion has been used as a tracer for methane sulfonic acid (MSA), which forms from the oxidation of marine dimethylsulfide emissions.⁶⁰ The area where these samples are collected is on a strip of land between the York River and the James River (about 6 miles away on each side), both of which empty into the Chesapeake Bay (Figure S1). Thus, marine-influenced particles are a possibility at this site. MSA would not be visible in the FT-ICR spectrum due to the mass range the instrument was tuned to. The chloride concentration in the samples was quite low (~0.02 g/L), and no correlation is observed between the samples with the CH_3SO_2^+ ion and higher chloride concentrations (Table 2). However, AMS is not quantitative for many alkali and alkaline earth salts due to their higher melting temperatures, so some chloride may not be measured well with this method. In addition, chloride has also been observed to volatilize out of dew water, and so it may be a poor tracer for marine influence.⁶¹ Chorine has also been observed in surface grime from road salting.^{10,62,63} However, there had been no snow fall in Virginia since the previous winter; thus, this is not expected to be an important source for these samples.

The CH_3SO_2^+ ion has also been found to form from organosulfates,⁶⁴ so it could be indicative of a larger total mass fraction of CHOS compounds in those samples. It may also be formed from other types of sulfonates like the ones that can be found in soil,⁶⁵ suggesting a different source for soil particles for those samples. Another difference between the FT-ICR data and the AMS spectra is the lack of any phosphate-containing ion fragments in the AMS spectra. This could indicate that the phosphate ions observed with FT-ICR are a small mass fraction of the sample. Future work will include ion chromatography to see if MSA is a component of these mixtures, or if other sulfates/sulfonates contribute to the CH_3SO_2^+ fragment. It will also include a characterization of

other phosphate-containing samples (organophosphates and phosphate salts) to better understand the instrument response.

AMS can also be used to measure the total concentration of organic matter in the samples. The concentrations of organics listed in Table 2 correspond to DOM, which includes all material in the samples (carbon, hydrogen, nitrogen, oxygen, and sulfur). For comparison with previous work, the concentration of dissolved organic carbon, or DOC, can be estimated using the measured organic mass to organic carbon ratio (OM/OC). The observed concentrations in Table 2 correspond to DOC concentrations of ~100 mg C L⁻¹. This is on the high end of DOC measured in dew water off clean surfaces⁵² and is similar to DOC concentrations in polluted cloud water.⁶⁶ The DOM measured here is the lower volatility material in the biogrime, most of which would be expected to remain on the surface after the dew dries in the morning. The concentration of the DOM is also expected to change as the dew droplets dry in the morning. Future work will target the volatile fraction for comparison with the lower volatility portion analyzed here and will include measurements of dew mass versus time.

Table 2 also lists the average values for the O/C, H/C, and N/C elemental ratios measured with AMS.⁶⁷ Compared to the FT-ICR data (Table 1), the O/C ratio is ~1.4–2 times larger in the AMS method, the H/C value is a little lower, and the N/C values are similar between the two methods. The application of offline-AMS to this type of sample is new, and it shows that the original dew water samples have a higher amount of oxidation compared to the extract measured with FT-ICR. One reason for this difference may be smaller molecules (less than 100 amu) which are not measured well with FT-ICR. Another option is the possibility that the original dew water may have a large mass fraction of sugars/carbohydrates. Prior work with DOM and offline-AMS demonstrated very good overlap between the elemental ratios measured via combustion analysis,³⁹ so it is likely that there are differences in the chemicals sampled and ionized here between the two methods. Here, insufficient sample was collected to compare the SPE extracted sample between both techniques (ESI/FT-ICR vs offline-AMS), but this comparison will be targeted in future experiments.

From the standpoint of dew water, it will be important to consider whether the DOM from the biogrime can enhance the dissolution of volatile organic compounds that deposit overnight. This enhancement has been observed for dew water samples off Teflon surfaces,^{31,32} which can have a lower overall DOC concentration due to the lack of a biogrime film. Much lower sorption would be expected for VOCs to chemicals like sugars compared to lignin due to the higher water solubility for sugars. The analysis presented here demonstrates that applying the total concentrations to the chemical properties measured with FT-ICR could overestimate the sorption behavior of these samples. Techniques like offline-AMS, which provide quantitative chemical properties of the full mixture, improve our

ability to model and predict the role biograde plays in enhanced dissolution of ROC into dew water and other surface water films in the biosphere.

3.3. UV/Vis Absorption and Photodecay. Organic chemicals found in dew water on leaf surfaces may experience multiple hydration/drying cycles, depending on when they are deposited/exuded. They can also be exposed to sunlight in the morning in the aqueous dew droplet, as well as throughout the day on the leaf surface. Many of the collected dew water solutions were brown/yellow in color, indicating that the material in the samples contained chromophores, or light-absorbing chemicals. UV/vis spectra for fresh dew water are shown in Figure 6a. Some samples had large enough

average absorptions (Bush and Sussex). This is consistent with the results from the offline-AMS analysis, showing concentrations below 0.1 g/L organic. The four other samples all have moderate absorption in the visible region (>350 nm) with the frost sample (purple) showing the most distinct absorption peak in this region. All four also show a peak around 280 nm, likely due to aromatics and carbonyls in the mixtures. The identities of the chromophores in these mixtures is unknown, but there may be contributions from dissolved soil organic matter and amino acids. The absorption features above 300 nm are larger than what was observed in Kroptavich et al. 2020, suggesting that the light-absorbing chemicals in these samples differ from those observed in urban grime samples.¹⁰

Any groups contributing to absorption in the visible region may be photoactive during sun exposure in the morning. Figure 6b shows the decrease in absorption measured from 360 to 365 nm for all six samples during photolysis with a xenon arc lamp. All data sets were fit with biexponential decays and showed initially rapid photodecay with lifetimes of ~0.5–2 h (Table 3). The light flux from the xenon arc lamp used here is very comparable to the solar light flux estimated with a solar zenith angle of 75° (Figure S2). This is approximately the angle expected in Williamsburg in the later fall months around 7 am, so the times observed here relate to what would be expected for dew droplets in these samples in the morning. The remaining color photobleached much more slowly in the cuvettes, indicating that some of the chromophores might be found on leaf surfaces for longer periods of time. The photolysis rates in dew water may not be the same as the rates for dry biograde films under direct sun during the day, so the total lifetime for the more photoresistant chromophores cannot be estimated here. In the cleaner samples (Bush and Sussex), a larger fraction of the signal decayed, suggesting that more photoresistant chromophores can build up with time after rainfall.

The rapid initial decays suggest the possibility for photolysis-driven chemistry in the dew droplets in the morning. Some of the longer-lived chromophores in the dew may be able to continue to drive indirect photolysis through excited triplet states in the chromophoric dissolved material.⁶⁸ Photoaging may influence the composition of the material dissolved in the droplets and could change the chemicals that volatilize after the dew droplets dry. The photobleaching observed here demonstrates one possible mechanism for the transformation of deposited ROC in the surface water films exposed to sunlight in the early morning.

4. CONCLUSIONS

Dew water collected off natural surfaces contains a very complex mixture of organic compounds with C, H, O, N, S,

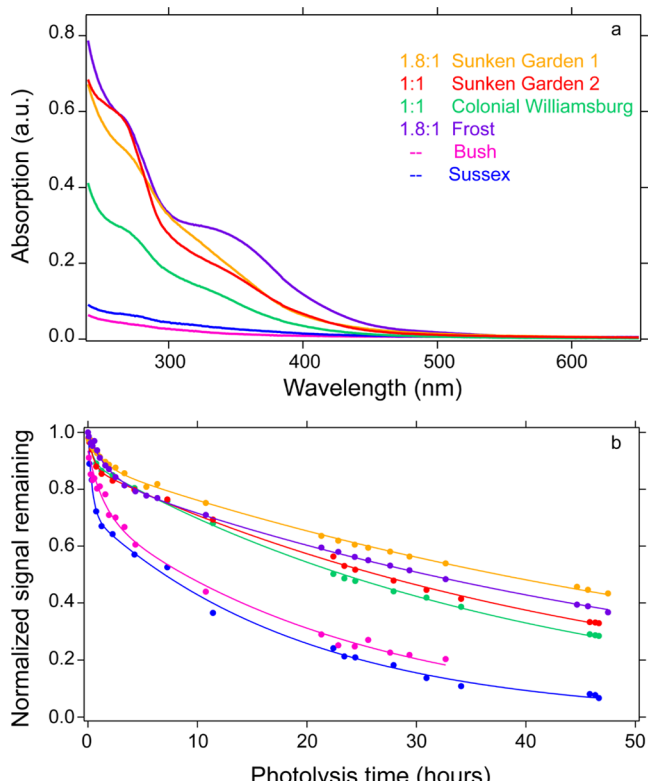


Figure 6. UV/vis data for the dew samples. (a) Initial absorption spectra with dilution volumes (mL) indicated in the label (sample/water), no dilution was needed for Bush or Sussex. (b) Decrease in absorption between 360 and 365 nm as a function of time. Lines represent biexponential fits for each sample.

absorption that dilution with Milli-Q water was necessary (see volumes in the figure legend). The two samples with cleaner mass spectra, collected after rainfall, had the lowest

Table 3. Biexponential Fits for the Photolysis-Driven Decrease in Absorption between 360 and 365 nm for Dew Water Samples^a

sample	A_1	τ_1 (h)	A_2	τ_2 (h)
Sunken Garden 1	0.10 ± 0.02	1.3 ± 0.2	0.89 ± 0.005	65 ± 1
Sunken Garden 2	0.12 ± 0.008	0.47 ± 0.09	0.88 ± 0.006	47 ± 0.7
Col. Williamsburg	0.10 ± 0.007	0.41 ± 0.08	0.90 ± 0.005	40 ± 0.5
Frost	0.15 ± 0.007	1.7 ± 0.2	0.85 ± 0.007	58 ± 1
Bush	0.21 ± 0.04	1.4 ± 0.6	0.72 ± 0.04	24 ± 2
Sussex	0.29 ± 0.02	0.38 ± 0.06	0.71 ± 0.01	20 ± 0.6

^aErrors are ± 1 standard deviation for the fits.

and P in the molecular formulas. FT-ICR spectra show intensity patterns characteristic of both DOM and aerosol particulate matter, and the elemental formulas found match chemicals from deposited particles/fog droplets and from metabolites (plant or microbiota). The different sources will vary in their contribution over time leading to a leaf surface “biogime” layer that builds and evolves after rainfalls. Offline-AMS provides a quantitative perspective on dew water composition and shows that sugars/carbohydrates are an important component by mass and that deposited marine-influenced aerosol particles may contribute to some of the films.

Samples collected at least a few days after rainfall were more complex than those collected after fresh rainfall, indicating that the material in the biogime films can wash off with rainfall. The dirtier samples contained chemicals with strong absorption in the visible region of the solar spectrum. All samples showed an initially rapid photodecay for absorption from 360 to 365 nm when irradiated with a xenon arc lamp, indicating that some of the organic material is photolabile. Depending on the composition of the dew water and the fragments produced during photolysis, photochemistry that occurs in the morning when the sun shines may be able to influence the composition of the volatilized material from drying dew droplets. The ability for these samples to absorb visible light suggests that they may also be able to drive photochemical reactions on the surface after the dew dries via processes such as photosensitization.⁶⁹

The composition of this material is important to understand because it may play a role in ROC flux out of the biosphere. Previous work has shown that dew can serve as a temporary reservoir for HONO or small volatiles like ammonia or isocyanic acid.^{9,29,70,71} Given the photoactivity of these mixtures, it is possible that some of the chemicals would be broken down and volatilized as the dew ages in the morning. In particular, the large number of nitrogen-containing compounds found here suggests that this type of material could be a source for volatile amines. Many of the chemicals in this mixture may also be bioactive and serve as a food source for microbes which can themselves emit VOCs.^{14,72}

Future work will target a wider range of natural surfaces, including those closer to urban areas and in forested environments, and will compare the organics and inorganics in natural surface samples to clean PTFE surface collections. More urban areas may have increased deposition of organic aerosol particles as well as increased NO_x and ozone, and forests may have increased deposition of OVOCs and hydrogen peroxide from BVOC oxidation products.⁶ Analysis of the mixtures with positive ion mode ESI will be carried out in addition to negative ion mode to provide more information on the nitrogen-containing ions. The chemical composition of samples during photolysis aging in the laboratory will also be measured and compared to the changes in the spectral shape with time in order to determine what types of chemicals are photoactive/photodegraded. The volatile organics released when either fresh or photoaged dew droplets dry on a surface will be characterized to provide more insight into the role biogime can play in the volatilization of material from surface water films.

This study provides a detailed characterization of the chemical composition, chemical properties, and photoaging rate for six dew water samples collected off leaf surfaces in Southeast Virginia. Previous studies in urban areas show that

outdoor surfaces can build up an “urban grime” layer of organic and inorganic compounds.^{10,11} In the biosphere, surfaces show a similar type of film, but there are additional sources from the plants themselves, as well as possibly microbes/fungi living on the leaf surfaces. We show that this biogime is a very complex mixture of organic compounds, and some components are photoactive, suggesting that this mixture can be a reactive site for transforming deposited ROC. In addition, components in the mixtures from plants/microbiome could fragment and volatilize, acting as a source for VOCs or amines/ammonia. Field and laboratory studies that investigate the role of these films in the partitioning and possible transformations of deposited compounds are needed to better understand the role surface biogime films play in biosphere/atmosphere exchange of ROC.

■ ASSOCIATED CONTENT

SI Supporting Information

The Supporting Information is available free of charge at <https://pubs.acs.org/doi/10.1021/acsearthspacechem.1c00445>.

Locations from which samples were collected, numbers of peaks identified for each type, the arc lamp spectrum, and AMS mass spectra for DNA standards (PDF)

Full peak list for the FT-ICR data sets (TXT)

■ AUTHOR INFORMATION

Corresponding Author

Rachel E. O'Brien — Department of Chemistry, William & Mary, Williamsburg, Virginia 23185, United States;
ORCID: orcid.org/0000-0001-8829-5517; Email: reobrien@wm.edu

Authors

Monica Dibley — Department of Chemistry, William & Mary, Williamsburg, Virginia 23185, United States

Aron Jaffe — Department of Chemistry, William & Mary, Williamsburg, Virginia 23185, United States

Complete contact information is available at: <https://pubs.acs.org/10.1021/acsearthspacechem.1c00445>

Author Contributions

M.D. and R.E.O.B. collected the samples, M.D. prepared the samples. M.D. and R.E.O.B. processed the data. M.D., R.E.O.B., and A.J. all assisted in the collection of the photoaging data set.

Notes

The authors declare no competing financial interest.

■ ACKNOWLEDGMENTS

This work was supported by the National Science Foundation under grant number AGS-2042619 and William & Mary Honors research funding. Acknowledgement is made to the Donors of the American Chemical Society Petroleum Research Fund for partial support of this research. The authors thank Jesse H. Kroll for granting access to the HR-ToF-AMS instrument and the use of the xenon arc lamp.

■ REFERENCES

- (1) Heald, C. L.; Kroll, J. H. The Fuel of Atmospheric Chemistry: Toward a Complete Description of Reactive Organic Carbon. *Sci. Adv.* **2020**, 6, No. eaay8967.

(2) Farmer, D. K.; Riches, M. Measuring Biosphere–Atmosphere Exchange of Short-Lived Climate Forcers and Their Precursors. *Acc. Chem. Res.* **2020**, *53*, 1427–1435.

(3) Kroll, J. H.; Seinfeld, J. H. Chemistry of Secondary Organic Aerosol: Formation and Evolution of Low-Volatility Organics in the Atmosphere. *Atmos. Environ.* **2008**, *42*, 3593–3624.

(4) Lee, S. H.; Gordon, H.; Yu, H.; Lehtipalo, K.; Haley, R.; Li, Y.; Zhang, R. New Particle Formation in the Atmosphere: From Molecular Clusters to Global Climate. *J. Geophys. Res.: Atmos.* **2019**, *124*, 7098–7146.

(5) Hallquist, M.; Wenger, J. C.; Baltensperger, U.; Rudich, Y.; Simpson, D.; Claeys, M.; Dommen, J.; Donahue, N. M.; George, C.; Goldstein, A. H.; Hamilton, J. F.; Herrmann, H.; Hoffmann, T.; Inuma, Y.; Jang, M.; Jenkin, M. E.; Jimenez, J. L.; Kiendler-Scharr, A.; Maenhaut, W.; McFiggans, G.; Mentel, T. F.; Monod, A.; Prevot, A. S. H.; Seinfeld, J. H.; Surratt, J. D.; Szmigielski, R.; Wildt, J. The Formation, Properties and Impact of Secondary Organic Aerosol: Current and Emerging Issues. *Atmos. Chem. Phys.* **2009**, *9*, 5155.

(6) Nguyen, T. B.; Crounse, J. D.; Teng, A. P.; St. Clair, J. M.; Paulot, F.; Wolfe, G. M.; Wennberg, P. O. Rapid Deposition of Oxidized Biogenic Compounds to a Temperate Forest. *Proc. Natl. Acad. Sci. U.S.A.* **2015**, *112*, E392–E401.

(7) Emerson, E. W.; Hodshire, A. L.; DeBolt, H. M.; Bilsback, K. R.; Pierce, J. R.; McMeeking, G. R.; Farmer, D. K. Revisiting Particle Dry Deposition and Its Role in Radiative Effect Estimates. *Proc. Natl. Acad. Sci. U.S.A.* **2020**, *117*, 26076–26082.

(8) Knote, C.; Hodzic, A.; Jimenez, J. L. The Effect of Dry and Wet Deposition of Condensable Vapors on Secondary Organic Aerosols Concentrations over the Continental US. *Atmos. Chem. Phys.* **2015**, *15*, 1–18.

(9) Fulgham, S. R.; Millet, D. B.; Alwe, H. D.; Goldstein, A. H.; Schobesberger, S.; Farmer, D. K. Surface Wetness as an Unexpected Control on Forest Exchange of Volatile Organic Acids. *Geophys. Res. Lett.* **2020**, *47*, No. e2020GL088745.

(10) Kropavich, C. R.; Zhou, S.; Kowal, S. F.; Kahan, T. F. Physical and Chemical Characterization of Urban Grime Sampled from Two Cities. *ACS Earth Space Chem.* **2020**, *4*, 1813–1822.

(11) Simpson, A. J.; Lam, B.; Diamond, M. L.; Donaldson, D. J.; Lefebvre, B. A.; Moser, A. Q.; Williams, A. J.; Larin, N. I.; Kvasha, M. P. Assessing the Organic Composition of Urban Surface Films Using Nuclear Magnetic Resonance Spectroscopy. *Chemosphere* **2006**, *63*, 142–152.

(12) Lam, B.; Diamond, M. L.; Simpson, A. J.; Makar, P. A.; Truong, J.; Hernandez-Martinez, N. A. Chemical Composition of Surface Films on Glass Windows and Implications for Atmospheric Chemistry. *Atmos. Environ.* **2005**, *39*, 6578–6586.

(13) Styler, S. A.; Baergen, A. M.; Donaldson, D. J.; Herrmann, H. Organic Composition, Chemistry, and Photochemistry of Urban Film in Leipzig, Germany. *ACS Earth Space Chem.* **2018**, *2*, 935–945.

(14) Misztal, P. K.; Lymeropoulou, D. S.; Adams, R. I.; Scott, R. A.; Lindow, S. E.; Bruns, T.; Taylor, J. W.; Uehling, J.; Bonito, G.; Vilgalys, R.; Goldstein, A. H. Emission Factors of Microbial Volatile Organic Compounds from Environmental Bacteria and Fungi. *Environ. Sci. Technol.* **2018**, *52*, 8272–8282.

(15) Netzker, T.; Shepherdson, E. M. F.; Zambri, M. P.; Elliot, M. A. Bacterial Volatile Compounds: Functions in Communication, Cooperation, and Competition. *Annu. Rev. Microbiol.* **2020**, *74*, 409–430.

(16) Baergen, A. M.; Donaldson, D. J. Formation of Reactive Nitrogen Oxides from Urban Grime Photochemistry. *Atmos. Chem. Phys.* **2016**, *16*, 6355–6363.

(17) Zhou, X.; Zhang, N.; TerAvest, M.; Tang, D.; Hou, J.; Bertman, S.; Alaghmand, M.; Shepson, P. B.; Carroll, M. A.; Griffith, S.; Dusander, S.; Stevens, P. S. Nitric Acid Photolysis on Forest Canopy Surface as a Source for Tropospheric Nitrous Acid. *Nat. Geosci.* **2011**, *4*, 440–443.

(18) Zhou, X.; Gao, H.; He, Y.; Huang, G.; Bertman, S. B.; Civerolo, K.; Schwab, J. Nitric Acid Photolysis on Surfaces in Low-NO_x Environments: Significant Atmospheric Implications. *Geophys. Res. Lett.* **2003**, *30*, 2217.

(19) Ide, J. i.; Ohashi, M.; Takahashi, K.; Sugiyama, Y.; Piirainen, S.; Kortelainen, P.; Fujitake, N.; Yamase, K.; Ohte, N.; Moritani, M.; Hara, M.; Finér, L. Spatial Variations in the Molecular Diversity of Dissolved Organic Matter in Water Moving through a Boreal Forest in Eastern Finland. *Sci. Rep.* **2017**, *7*, 42102.

(20) Stubbins, A.; Silva, L. M.; Dittmar, T.; Van Stan, J. T. Molecular and Optical Properties of Tree-Derived Dissolved Organic Matter in Throughfall and Stemflow from Live Oaks and Eastern Red Cedar. *Front. Earth Sci.* **2017**, *5*, 22.

(21) Thieme, L.; Graeber, D.; Hofmann, D.; Bischoff, S.; Schwarz, M. T.; Steffen, B.; Meyer, U.-N.; Kaupenjohann, M.; Wilcke, W.; Michalzik, B.; Siemens, J. Dissolved Organic Matter Characteristics of Deciduous and Coniferous Forests with Variable Management: Different at the Source, Aligned in the Soil. *Biogeosciences* **2019**, *16*, 1411–1432.

(22) Van Stan, J. T.; Stubbins, A. Tree-DOM: Dissolved Organic Matter in Throughfall and Stemflow. *Limnol. Oceanogr. Lett.* **2018**, *3*, 199–214.

(23) Chiwa, M.; Miyake, T.; Kimura, N.; Sakugawa, H. Organic Acids and Aldehydes in Throughfall and Dew in a Japanese Pine Forest. *J. Environ. Qual.* **2008**, *37*, 2397–2402.

(24) Grant, J. S.; Zhu, Z.; Anderton, C. R.; Shaw, S. K. Physical and Chemical Morphology of Passively Sampled Environmental Films. *ACS Earth Space Chem.* **2019**, *3*, 305–313.

(25) Grant, J. S.; Richards, P. M.; Anderton, C. R.; Zhu, Z.; Mattes, T. E.; Shaw, S. K. Passively Sampled Environmental Films Show Geographic Variability and Host a Variety of Microorganisms. *ACS Earth Space Chem.* **2019**, *3*, 2726–2735.

(26) Monteith, J. L. Dew. *Q. J. R. Meteorol. Soc.* **1957**, *83*, 322–341.

(27) Matsumoto, K.; Kawai, S.; Igawa, M. Dominant Factors Controlling Concentrations of Aldehydes in Rain, Fog, Dew Water, and in the Gas Phase. *Atmos. Environ.* **2005**, *39*, 7321–7329.

(28) Takeuchi, M.; Okochi, H.; Igawa, M. Deposition of Coarse Soil Particles and Ambient Gaseous Components Dominating Dew Water Chemistry. *J. Geophys. Res.* **2003**, *108*, 4319.

(29) Wentworth, G. R.; Murphy, J. G.; Benedict, K. B.; Bangs, E. J.; Collett, J. L., Jr. The Role of Dew as a Night-Time Reservoir and Morning Source for Atmospheric Ammonia. *Atmos. Chem. Phys.* **2016**, *16*, 7435–7449.

(30) Shohel, M.; Simol, H. A.; Reid, E.; Reid, J. S.; Salam, A. Dew Water Chemical Composition and Source Characterization in the IGP Outflow Location (Coastal Bhola, Bangladesh). *Air Qual., Atmos. Health* **2017**, *10*, 981–990.

(31) Okochi, H.; Kataniwa, M.; Sugimoto, D.; Igawa, M. Enhanced Dissolution of Volatile Organic Compounds into Urban Dew Water Collected in Yokohama, Japan. *Atmos. Environ.* **2005**, *39*, 6027–6036.

(32) Okochi, H.; Sato, E.; Matsubayashi, Y.; Igawa, M. Effect of Atmospheric Humic-like Substances on the Enhanced Dissolution of Volatile Organic Compounds into Dew Water. *Atmos. Res.* **2008**, *87*, 213–223.

(33) Nguyen, T. B.; Lee, P. B.; Updyke, K. M.; Bones, D. L.; Laskin, J.; Laskin, A.; Nizkorodov, S. A. Formation of Nitrogen- and Sulfur-Containing Light-Absorbing Compounds Accelerated by Evaporation of Water from Secondary Organic Aerosols: BROWN CARBON FROM DROPLET EVAPORATION. *J. Geophys. Res.: Atmos.* **2012**, *117*, D01207.

(34) George, C.; Ammann, M.; D'Anna, B.; Donaldson, D. J.; Nizkorodov, S. A. Heterogeneous Photochemistry in the Atmosphere. *Chem. Rev.* **2015**, *115*, 4218–4258.

(35) Simon, C.; Roth, V.-N.; Dittmar, T.; Gleixner, G. Molecular Signals of Heterogeneous Terrestrial Environments Identified in Dissolved Organic Matter: A Comparative Analysis of Orbitrap and Ion Cyclotron Resonance Mass Spectrometers. *Front. Earth Sci.* **2018**, *6*, 138.

(36) Xu, W.; Gao, Q.; He, C.; Shi, Q.; Hou, Z.-Q.; Zhao, H.-Z. Using ESI FT-ICR MS to Characterize Dissolved Organic Matter in

Salt Lakes with Different Salinity. *Environ. Sci. Technol.* **2020**, *54*, 12929–12937.

(37) Li, Y.; Harir, M.; Lucio, M.; Kanawati, B.; Smirnov, K.; Flerus, R.; Koch, B. P.; Schmitt-Kopplin, P.; Hertkorn, N. Proposed Guidelines for Solid Phase Extraction of Suwannee River Dissolved Organic Matter. *Anal. Chem.* **2016**, *88*, 6680–6688.

(38) DeCarlo, P. F.; Kimmel, J. R.; Trimborn, A.; Northway, M. J.; Jayne, J. T.; Aiken, A. C.; Gonin, M.; Fuhrer, K.; Horvath, T.; Docherty, K. S.; Worsnop, D. R.; Jimenez, J. L. Field-Deployable, High-Resolution, Time-of-Flight Aerosol Mass Spectrometer. *Anal. Chem.* **2006**, *78*, 8281–8289.

(39) O'Brien, R. E.; Ridley, K. J.; Canagaratna, M. R.; Jayne, J. T.; Croteau, P. L.; Worsnop, D. R.; Budisulistiorini, S. H.; Surratt, J. D.; Follett, C. L.; Repeta, D. J.; Kroll, J. H. Ultrasonic Nebulization for the Elemental Analysis of Microgram-Level Samples with Offline Aerosol Mass Spectrometry. *Atmos. Meas. Tech.* **2019**, *12*, 1659–1671.

(40) Stubbins, A.; Spencer, R. G. M.; Chen, H.; Hatcher, P. G.; Mopper, K.; Hernes, P. J.; Mwamba, V. L.; Mangangu, A. M.; Wabakanganzi, J. N.; Six, J. Illuminated Darkness: Molecular Signatures of Congo River Dissolved Organic Matter and Its Photochemical Alteration as Revealed by Ultrahigh Precision Mass Spectrometry. *Limnol. Oceanogr.* **2010**, *55*, 1467–1477.

(41) Lawson, E. C.; Bhatia, M. P.; Wadham, J. L.; Kujawinski, E. B. Continuous Summer Export of Nitrogen-Rich Organic Matter from the Greenland Ice Sheet Inferred by Ultrahigh Resolution Mass Spectrometry. *Environ. Sci. Technol.* **2014**, *48*, 14248–14257.

(42) Canagaratna, M. R.; Jimenez, J. L.; Kroll, J. H.; Chen, Q.; Kessler, S. H.; Massoli, P.; Hildebrandt Ruiz, L.; Fortner, E.; Williams, L. R.; Wilson, K. R.; Surratt, J. D.; Donahue, N. M.; Jayne, J. T.; Worsnop, D. R. Elemental Ratio Measurements of Organic Compounds Using Aerosol Mass Spectrometry: Characterization, Improved Calibration, and Implications. *Atmos. Chem. Phys.* **2015**, *15*, 253–272.

(43) Bahureksa, W.; Tfaily, M. M.; Boiteau, R. M.; Young, R. B.; Logan, M. N.; McKenna, A. M.; Borch, T. Soil Organic Matter Characterization by Fourier Transform Ion Cyclotron Resonance Mass Spectrometry (FTICR MS): A Critical Review of Sample Preparation, Analysis, and Data Interpretation. *Environ. Sci. Technol.* **2021**, *55*, 9637–9656.

(44) Guigue, J.; Harir, M.; Mathieu, O.; Lucio, M.; Ranjard, L.; Lévéque, J.; Schmitt-Kopplin, P. Ultrahigh-Resolution FT-ICR Mass Spectrometry for Molecular Characterisation of Pressurised Hot Water-Extractable Organic Matter in Soils. *Biogeochemistry* **2016**, *128*, 307–326.

(45) Pospisilova, V.; Lopez-Hilfiker, F. D.; Bell, D. M.; El Haddad, I.; Mohr, C.; Huang, W.; Heikkinen, L.; Xiao, M.; Dommen, J.; Prevot, A. S. H.; Baltensperger, U.; Slowik, J. G. On the Fate of Oxygenated Organic Molecules in Atmospheric Aerosol Particles. *Sci. Adv.* **2020**, *6*, No. eaax8922.

(46) Walhout, E. Q.; Yu, H.; Thrasher, C.; Shusterman, J. M.; O'Brien, R. E. Effects of Photolysis on the Chemical and Optical Properties of Secondary Organic Material Over Extended Time Scales. *ACS Earth Space Chem.* **2019**, *3*, 1226–1236.

(47) Reinhardt, A.; Emmenegger, C.; Gerrits, B.; Panse, C.; Dommen, J.; Baltensperger, U.; Zenobi, R.; Kalberer, M. Ultrahigh Mass Resolution and Accurate Mass Measurements as a Tool To Characterize Oligomers in Secondary Organic Aerosols. *Anal. Chem.* **2007**, *79*, 4074–4082.

(48) Polkowska, Ž.; Błaś, M.; Klimaszewska, K.; Sobik, M.; Malek, S.; Namięśnik, J. Chemical Characterization of Dew Water Collected in Different Geographic Regions of Poland. *Sensors* **2008**, *8*, 4006–4032.

(49) Xu, Y.; Zhu, H.; Tang, J.; Lin, Y. Chemical Compositions of Dew and Scavenging of Particles in Changchun, China. *Adv. Meteorol.* **2015**, *2015*, 1–11.

(50) Nath, S.; Yadav, S. A Comparative Study on Fog and Dew Water Chemistry at New Delhi, India. *Aerosol Air Qual. Res.* **2018**, *18*, 26–36.

(51) Beysens, D.; Mongruel, A.; Acker, K. Urban Dew and Rain in Paris, France: Occurrence and Physico-Chemical Characteristics. *Atmos. Res.* **2017**, *189*, 152–161.

(52) Takeuchi, M.; Okochi, H.; Igawa, M. Controlling Factors of Weak Acid and Base Concentrations in Urban Dewwater—Comparison of Dew Chemistry with Rain and Fog Chemistry. *Bull. Chem. Soc. Jpn.* **2002**, *75*, 757–764.

(53) Wozniak, A. S.; Bauer, J. E.; Sleighter, R. L.; Dickhut, R. M.; Hatcher, P. G. Technical Note: Molecular Characterization of Aerosol-Derived Water Soluble Organic Carbon Using Ultrahigh Resolution Electrospray Ionization Fourier Transform Ion Cyclotron Resonance Mass Spectrometry. *Atmos. Chem. Phys.* **2008**, *8*, 5099–5111.

(54) O'Brien, R. E.; Laskin, A.; Laskin, J.; Rubitschun, C. L.; Surratt, J. D.; Goldstein, A. H. Molecular Characterization of S- and N-Containing Organic Constituents in Ambient Aerosols by Negative Ion Mode High-Resolution Nanospray Desorption Electrospray Ionization Mass Spectrometry: CalNex 2010 Field Study. *J. Geophys. Res.: Atmos.* **2014**, *119*, 12706.

(55) O'Brien, R. E.; Laskin, A.; Laskin, J.; Liu, S.; Weber, R.; Russell, L. M.; Goldstein, A. H. Molecular Characterization of Organic Aerosol Using Nanospray Desorption/Electrospray Ionization Mass Spectrometry: CalNex 2010 Field Study. *Atmos. Environ.* **2013**, *68*, 265–272.

(56) Smith, P. B. W.; Snyder, A. P.; Harden, C. S. Characterization of Bacterial Phospholipids by Electrospray Ionization Tandem Mass Spectrometry. *Anal. Chem.* **1995**, *67*, 1824–1830.

(57) Urbaneja-Bernat, P.; Tena, A.; González-Cabrera, J.; Rodriguez-Saona, C. Plant Guttation Provides Nutrient-Rich Food for Insects. *Proc. R. Soc. B* **2020**, *287*, 20201080.

(58) Farmer, D. K.; Boedicker, E. K.; DeBolt, H. M. Dry Deposition of Atmospheric Aerosols: Approaches, Observations, and Mechanisms. *Annu. Rev. Phys. Chem.* **2021**, *72*, 375–397.

(59) Raeke, J.; Lechtenfeld, O. J.; Wagner, M.; Herzsprung, P.; Reemtsma, T. Selectivity of Solid Phase Extraction of Freshwater Dissolved Organic Matter and Its Effect on Ultrahigh Resolution Mass Spectra. *Environ. Sci.: Processes Impacts* **2016**, *18*, 918–927.

(60) Zorn, S. R.; Drewnick, F.; Schott, M.; Hoffmann, T.; Borrmann, S. Characterization of the South Atlantic Marine Boundary Layer Aerosol Using an Aerodyne Aerosol Mass Spectrometer. *Atmos. Chem. Phys.* **2008**, *8*, 4711.

(61) Takenaka, N.; Takayama, K.; Ojiro, N.; Shimazaki, W.; Ohira, K.; Soda, H.; Suzue, T.; Sadanaga, Y.; Bandow, H.; Maeda, Y. The Chemistry of Drying an Aqueous Solution of Salts. *J. Phys. Chem. A* **2009**, *113*, 12233–12242.

(62) Baergen, A. M.; Donaldson, D. J. Seasonality of the Water-Soluble Inorganic Ion Composition and Water Uptake Behavior of Urban Grime. *Environ. Sci. Technol.* **2019**, *53*, 5671–5677.

(63) DeYoung, J. L.; Holyoake, E. A.; Shaw, S. K. What Are the Differences between Two Environmental Films Sampled 1 Km Apart? *ACS Earth Space Chem.* **2021**, *5*, 3407–3413.

(64) Farmer, D. K.; Matsunaga, A.; Docherty, K. S.; Surratt, J. D.; Seinfeld, J. H.; Ziemann, P. J.; Jimenez, J. L.; Finlayson-Pitts, B. J. Response of an Aerosol Mass Spectrometer to Organonitrates and Organosulfates and Implications for Atmospheric Chemistry. *Proc. Natl. Acad. Sci. U.S.A.* **2010**, *107*, 6670–6675.

(65) Autry, A. R.; FitzgeraldSulfonate, J. W. S. A Major Form of Forest Soil Organic Sulfur. *Biol. Fertil. Soils* **1990**, *10*, 50–56.

(66) Herkes, P.; Valsaraj, K. T.; Collett, J. L. A Review of Observations of Organic Matter in Fogs and Clouds: Origin, Processing and Fate. *Atmos. Res.* **2013**, *132–133*, 434–449.

(67) Aiken, A. C.; DeCarlo, P. F.; Kroll, J. H.; Worsnop, D. R.; Huffman, J. A.; Docherty, K. S.; Ulbrich, I. M.; Mohr, C.; Kimmel, J. R.; Sueper, D.; Sun, Y.; Zhang, Q.; Trimborn, A.; Northway, M.; Ziemann, P. J.; Canagaratna, M. R.; Onasch, T. B.; Alfarra, M. R.; Prevot, A. S. H.; Dommen, J.; Duplissy, J.; Metzger, A.; Baltensperger, U.; Jimenez, J. L. O/C and OM/OC Ratios of Primary, Secondary, and Ambient Organic Aerosols with High-Resolution Time-of-Flight

Aerosol Mass Spectrometry. *Environ. Sci. Technol.* **2008**, *42*, 4478–4485.

(68) McNeill, K.; Canonica, S. Triplet State Dissolved Organic Matter in Aquatic Photochemistry: Reaction Mechanisms, Substrate Scope, and Photophysical Properties. *Environ. Sci.: Processes Impacts* **2016**, *18*, 1381–1399.

(69) McNeill, V. F.; Ariya, P. A., Eds. In *Atmospheric and Aerosol Chemistry*; Springer Berlin Heidelberg; Topics in Current Chemistry: Berlin, Heidelberg, 2014; Vol. 339.

(70) Zhou, X.; Civerolo, K.; Dai, H.; Huang, G.; Schwab, J.; Demerjian, K. Summertime Nitrous Acid Chemistry in the Atmospheric Boundary Layer at a Rural Site in New York State. *J. Geophys. Res. Atmos.* **2002**, *107*, 13.

(71) Ren, Y.; Stieger, B.; Spindler, G.; Grosselin, B.; Mellouki, A.; Tuch, T.; Wiedensohler, A.; Herrmann, H. Role of the Dew Water on the Ground Surface in HONO Distribution: A Case Measurement in Melpitz. *Atmos. Chem. Phys.* **2020**, *20*, 13069.

(72) McBride, S. G.; Choudoir, M.; Fierer, N.; Strickland, M. S. Volatile Organic Compounds from Leaf Litter Decomposition Alter Soil Microbial Communities and Carbon Dynamics. *Ecology* **2020**, *101*(1). <https://doi.org/10.1002/ecy.3130>. DOI: 10.1002/ecy.3130

□ Recommended by ACS

Morphology and Viscosity Changes after Reactive Uptake of Isoprene Epoxides in Submicrometer Phase Separated Particles with Secondary Organic Aerosol ...

Ziying Lei, Andrew P. Ault, et al.

MARCH 23, 2022

ACS EARTH AND SPACE CHEMISTRY

READ ▶

Production of Peroxy Radicals from the Photochemical Reaction of Fatty Acids at the Air–Water Interface

Nathalie Hayeck, Christian George, et al.

JULY 20, 2020

ACS EARTH AND SPACE CHEMISTRY

READ ▶

Impact of Tetrabutylammonium on the Oxidation of Bromide by Ozone

Shuzhen Chen, Markus Ammann, et al.

OCTOBER 26, 2021

ACS EARTH AND SPACE CHEMISTRY

READ ▶

Ozonolysis of Oleic Acid Aerosol Revisited: Multiphase Chemical Kinetics and Reaction Mechanisms

Thomas Berkemeier, Ulrich Pöschl, et al.

NOVEMBER 19, 2021

ACS EARTH AND SPACE CHEMISTRY

READ ▶

[Get More Suggestions >](#)